Projection-Compliant Database Generation

Anupam Sanghi
Database Systems Lab
Indian Institute of Science
anupamsanghi@iisc.ac.in

Shadab Ahmed
Database Systems Lab
Indian Institute of Science
shadabahmed@iisc.ac.in

Jayant R. Haritsa
Database Systems Lab
Indian Institute of Science
haritsa@iisc.ac.in

ABSTRACT

Synthesizing data using declarative formalisms has been persuasively advocated in contemporary data generation frameworks. In particular, they specify operator output volumes through row-cardinality constraints. However, thus far, adherence to these volumetric constraints has been limited to the Filter and Join operators. A critical deficiency is the lack of support for the Projection operator, which is at the core of basic SQL constructs such as Distinct, Union and Group By. The technical challenge here is that cardinality *unions* in multi-dimensional space, and not mere summations, need to be captured in the generation process. Further, dependencies *across* different data subspaces need to be taken into account.

We address the above lacuna by presenting **PiGen**, a dynamic data generator that incorporates Projection cardinality constraints in its ambit. The design is based on a projection subspace division strategy that supports the expression of constraints using optimized linear programming formulations. Further, techniques of symmetric refinement and workload decomposition are introduced to handle constraints across different projection subspaces. Finally, PiGen supports dynamic generation, where data is generated on-demand during query processing, making it amenable to Big Data environments. A detailed evaluation on workloads derived from real-world and synthetic benchmarks demonstrates that PiGen can accurately and efficiently model Projection outcomes, representing an essential step forward in customized database generation.

PVLDB Reference Format:
Anupam Sanghi, Shadab Ahmed, and Jayant R. Haritsa.
Projection-Compliant Database Generation. PVLDB, 15(5): 998 - 1010, 2022.
doi:10.14778/3510397.3510398

PVLDB Artifact Availability:
The source code, data, and/or other artifacts have been made available at https://dsl.cds.iisc.ac.in/projects/HYDRA/index.html.

1 INTRODUCTION

Synthetic databases are required in a variety of use-cases, ranging from testing and tuning of database engines and applications to system benchmarking. In the past decade, several frameworks (e.g. [8, 14, 18, 23]) have advocated data synthesis using a set of cardinality constraints. In particular, a *cardinality constraint* dictates that the output of a given relational expression over the generated database should feature a specified number of rows. For SPJ query formulations, the canonical constraint representation is:

$$|\pi_{\mathbb{A}}(\sigma_f(T_1 \bowtie T_2 \bowtie ... \bowtie T_N))| = k$$

where f represents the *filter predicates* applied on the inner join of a group of tables $T_1, ...T_N$ in the database; $\mathbb{A}$ represents the *projection-attribute-set*, i.e. the set of attributes on which the projection is applied; and k is a count representing the output row-cardinality of the relational expression. The provenance of these constraints could be either from construction of *what-if* scenarios, or based on information sourced from an actual client installation – for instance, Annotated Query Plans [11]. Further, the constraints could be *parameterized* wrt predicate constants [18, 19], or more commonly in industrial practice, *strict*, where even these constants are prespecified [8, 23].

Generating synthetic data that adheres to a collection of strict cardinality constraints was first proposed in the pioneering work of **DataSynth** [8, 9]. This initial effort was later extended in **Hydra** [23, 24] to incorporate dynamism and scale in the generation process. The key idea in these frameworks is to express the input constraints using a *linear feasibility program* (LP), and then use the LP solution to construct the synthetic database. While these prior frameworks accurately and efficiently handle an important class of cardinality constraints, a critical lacuna is support for the *projection* operator. In this paper, we investigate the explicit incorporation of Projection into the data generation framework.

1.1 Incorporating Projections

Our motivation for modeling Projection stems from its core appearance in the Distinct, Group By, and Union SQL constructs – as a case in point, among the 22 queries in the TPC-H benchmark [5], as many as 16 feature the projection operation. Further, projection-compliant databases can be beneficial to database vendors in a variety of use-cases as listed in [21] (and verified with industry experts in a recent Dagstuhl Seminar [1]). Among these, a particularly compelling use-case is in the context of engine upgrades, where a critical requirement is to synthesize data that can mimic client environments for *regression testing*. This facility enables: (a) Catching optimizer bugs such as a change in query plan leading to performance degradation, or incorrect query rewriting leading to erroneous query results; (b) Performance evaluation of operators in the query execution pipeline. For instance, a thorough assessment of a new memory manager's ability to handle native projection-based operators (e.g. hash aggregate, sort) is predicated on accurate modeling of projection cardinalities; and (c) Given an operator of interest, evaluating its impact on the performance of downstream operations. For instance, in the 16 projection-featuring queries of TPC-H, 12 require a sort operation immediately following projection. Further, in 4 queries, the projection output serves as

Proceedings of the VLDB Endowment, Vol. 15, No. 5 ISSN 2150-8097.
doi:10.14778/3510397.3510398

an intermediate staging for subsequent filter/join operations. In all these cases, the projection output cardinality affects the behavior of the downstream operations.

Apart from regression testing, another common use-case arises in the context of *system benchmarking*, when evaluating competing database platforms for hosting an application.

Our focus here is on the *duplicate-eliminating* version of projection where only the *distinct* rows are retained in the projected output (the alternative duplicate-preserving option does not alter the filter output's row-cardinality, and is therefore trivially handled by the existing frameworks). Additionally, since projection is a unary operator, we present the ideas using a single-table environment. To handle multi-relation environments, we can take recourse to the methodology of [8, 23], where denormalized relations are constructed as an intermediate step in the solution process.

1.2 Projection-inclusive Constraint (PIC)

To represent a projection-inclusive cardinality constraint c on a table $\mathcal{T}$, we use the quadruple $\mathbf{c} : \langle \mathbf{f}, \mathbb{A}, \mathbf{l}, \mathbf{k} \rangle$, as a shorthand notation. Here, f represents the filter predicate applied on $\mathcal{T}$, $\mathbb{A}$ represents the projection attribute-set (PAS), l signifies the row-cardinality of the filtered table, and k represents the row-cardinality after projection on this filtered table.

As as sample instance, consider the following set of PICs on a generated table Purchases (PID, Qty, Amt, $Year$):

$c_1 : \langle f_1, Amt, 500, \mathbf{5} \rangle \mid f_1 = (Qty < 20) \wedge (1100 \leq Amt < 2500)$

$c_2 : \langle f_2, Amt, 1000, \mathbf{3} \rangle \mid f_2 = (Qty \geq 20) \wedge (500 \leq Amt < 3000)$

$c_3 : \langle f_3, Qty, 3000, \mathbf{9} \rangle \mid f_3 = (Qty \geq 10)$

Here, PIC c_1 denotes that applying the f_1 predicate on Purchases should produce 500 rows in the output, which is further reduced to 5 rows after projecting on the Amt column; the other PICs can be interpreted analogously.

1.3 Technical Challenges

There are two primary challenges to modeling PICs within the table generation process, related to handling dependencies within and across the data subspaces identified by these constraints, as described below.

Intra-Projection Subspace Dependencies. Consider the projection subspace spanned by a set of attributes $\mathbb{A}$. Dealing with projection requires computing union of groups of tuples. For example, for two tuples/group of tuples b_1 and b_2, the direct expression for computing projection along $\mathbb{A}$ is:

$$|\pi_{\mathbb{A}}(b_1 \cup b_2)|$$

However, even if b_1 and b_2 are disjoint in the original table, their projections onto $\mathbb{A}$ may *overlap*. Therefore, to handle PICs, explicitly computing the cardinality of the *union* of a group of tuples post-projection is required. Using the fact that projection distributes over union [26], we can rewrite the above expression as:

$$|\pi_{\mathbb{A}}(b_1) \cup \pi_{\mathbb{A}}(b_2)|$$

but even here the union does not translate to a simple summation. For instance, consider the following two sample rows from the Purchases table:

u : (PID = 10001, Amt = 1500, Qty = 3, $Year$ = 2020), and
v : (PID = 10002, Amt = 1500, Qty = 16, $Year$ = 2021).

Both rows satisfy the filter f_1, but the union of their projections along Amt yields a single outcome – namely, Amt = 1500.

Inter-Projection Subspace Dependencies. When a set of tuples b is subjected to multiple projections, the data generation for projection subspaces may be interdependent. Given a pair of PASs $\mathbb{A}_1$ and $\mathbb{A}_2$, sourced from two PICs, we have the inclusion property:

$$\pi_{\mathbb{A}_1 \cup \mathbb{A}_2}(b) \subseteq \pi_{\mathbb{A}_1}(b) \times \pi_{\mathbb{A}_2}(b)$$

For instance, consider a group of tuples b, from the table $Purchases$, satisfying the following disjunctive filter condition:

$$b = \{t \in Purchases \mid (t.Qty \geq 20 \wedge t.Amt \geq 3000) \vee (10 \leq t.Qty < 20 \wedge t.Amt \geq 2500)\}$$

Here, a tuple with Amt = 2700 and Qty = 25 can belong to both $\pi_{Amt}(b)$ and $\pi_{Qty}(b)$, but lies outside b's boundary.

Moreover, $\mathbb{A}_1$ and $\mathbb{A}_2$ may themselves intersect. Therefore, in general, expressing a set of PICs with an LP, while ensuring a physically constructible solution, is often infeasible – this is because the set of constructible solutions does not form a convex polytope [16]. Hence, alternative methods are needed to address this issue.

1.4 Our Contributions

We present here **PiGen**, a data generator that addresses the above challenges and extends the current scope of data generation to include projection in its ambit. The key design principles are: (a) *Projection Subspace Division*, which divides each projection subspace into regions that allow modeling the unions, thereby ensuring that the intra-subspace dependencies are resolved; and (b) *Isolating Projections*, for independent processing of each projection subspace, thereby tackling the inter-projection subspace challenge.

Additionally, PiGen leverages the concept of *dynamic regeneration* [23], and constructs an *Enriched Table Summary*, that ensures data can be generated on-demand during query processing while satisfying the input PICs. Therefore, no materialized table is required in the entire testing pipeline. Further, the time and space overheads incurred in constructing the summary is independent of the size of the table to be constructed and, in our evaluations, requires only a few 100 KBs of storage.

A detailed evaluation on multiple workloads of PICs, covering both real-world datasets (IMDB, Census), and synthetic benchmarks (TPC-DS) has been conducted. The results demonstrates that PiGen accurately and efficiently models Projection outcomes. As a case in point, for a workload of PICs, comprising over a hundred PICs in total, PiGen generated data that satisfied all the PICs, with *perfect accuracy*. Moreover, the entire summary production pipeline completed within viable time and space overheads.

Organization. The remainder of the paper is organized as follows: The prior literature is reviewed in Section 2. The problem framework is discussed in Section 3. Further, the key design principles of PiGen are introduced in Section 4, and then described in detail in Sections 5 through 8. The end-to-end implementation pipeline is presented in Section 9, while the experimental evaluation is reported in Section 10. Finally, our conclusions and future research avenues are summarized in Section 11.

2 RELATED WORK

Over the past three decades, a variety of novel approaches have been proposed for synthetic database generation. The initial efforts (e.g. [13, 15]) focused on generating databases using standard mathematical distributions. Subsequently, data generation techniques that incorporated the notion of constraints were proposed – for instance, adherence to a given set of metadata statistics was addressed in [7, 20, 25]. In more recent times, generation techniques driven by constraints on query outputs have been analyzed. A particularly potent effort in this class was **RQP** [10], which receives a query and a result as input, and returns a minimal database instance that produces the same result for the query. An alternative fine-grained constraint formulation is to specify the row-cardinalities of the individual operator outputs, and the techniques advocated in [8, 11, 14, 18, 19, 22, 23] fall in this category. They can be classified into two groups based on the nature of constraints. In the first group, parameterized constraints form the input in **QAGen** [11], **MyBenchmark** [19] and **TouchStone** [18]. That is, the predicate constants are variables. From these constraints, these techniques generate a synthetic database and predicate instantiations, such that applying the instantiated constraints on the synthetic data produces the desired number of rows.

On the other hand, a stricter notion of fixed constraints was considered in [8, 14, 22, 23], where the predicate constants are prespecified in the input. This strict model helps to generate data that is (a) more directly representative of the source environment, and as a consequence (b) more robust to future queries outside of the original workload. However, while constraints with filter and join operators have been handled satisfactorily, support for the projection operator has been minimal, restricted to a few extreme cases. For instance, **DataSynth** [8] proposed a projection generator that catered to *single-column* tables. Here, due to the single-column restriction, there are by definition no intra/inter projection subspace dependencies. In contrast, in PiGen, we consider a general class of strict PICs, requiring us to explicitly address these challenges.

Complementary to these database studies, the mathematical literature includes work such as [12, 16, 27] that study conditions for ensuring feasibility of a given set of projection constraints. However, they do not adequately address our requirements, as discussed in detail in Section 9 (PiGen deployment).

3 PROBLEM FRAMEWORK

In this section, we summarize the basic problem statement, and the underlying assumptions of our PiGen solution.

Statement. Given an input table schema S and a workload $\mathbb{W}$ of strict PICs on S, the objective of data generation is to construct a table $\mathcal{T}$, such that it conforms to S and satisfies $\mathbb{W}$.

Assumptions. We assume that each PIC in $\mathbb{W}$ is of the form described in the Introduction, and that it is strict (i.e., with prespecified predicate constants). Further, for ease of presentation, we assume that $\mathbb{W}$ is *collectively feasible*, that is, there exists at least one legal database instance satisfying all the constraints – the infeasibility scenario is deferred to Section 9. Finally, for brevity, we present the ideas using tables with *continuous numeric* columns; the extension to other data types is straightforward.

Output. Given S and $\mathbb{W}$, PiGen outputs a collection of table summaries. Each summary $s(\mathcal{T})$ can be used to deterministically produce the associated table $\mathcal{T}$. The tables produced are such that: (a) all of them conform to S, and (b) each input PIC in $\mathbb{W}$ is satisfied by at least one of them.

Notations. The main acronyms and key notations used in the rest of the paper are summarized in Tables 1 and 2, respectively.

Table 1: Acronyms

Acronym	Meaning
PAS	Projection Attribute Set
PIC	Projection-inclusive Cardinality Constraint
FB	Filter Block
RB	Refined Block
PRB	Projected Refined Block
CPB	Constituent Projection Block
PSD	Projection Subspace Division

Table 2: Notations

(a) **Input Related**

Symbol	Meaning
S	Table Schema
f	Filter predicate
$\mathbb{A}$	A PAS
l	Output row cardinality of a filtered table
k	Output row cardinality after projecting on a PAS
c	A PIC $\langle f, \mathbb{A}, l, k\rangle$
$\mathbb{W}$	Input PICs workload
$\mathbb{C}$	A compatible PICs workload

(b) **Output Table Related**

Symbol	Meaning
$\mathcal{T}$	Output Table
$s(\mathcal{T})$	Summary of $\mathcal{T}$
$\mathbb{U}$	attribute-set in $\mathcal{T}$
$\mathbb{D}$	Data space of $\mathcal{T}$
$\mathbb{D}^{\mathbb{A}}$	Data subspace spanned by $\mathbb{A}$

(c) **Block Related**

Symbol	Meaning
b	An FB
$\mathbb{R}$	Set of all RBs
r	An RB
$\overline{r}$	PRB wrt r and some PAS
$\overline{\mathbb{R}}^{\mathbb{A}}$	Set of PRBs for $\mathbb{A}$
p	A CPB
$\mathbb{P}^{\mathbb{A}}$	Set of CPBs for $\mathbb{A}$
x_r	variable for $\lvert r\rvert$
y_p	variable for $\lvert p\rvert$

(d) **Relation Related**

Symbol	Meaning
M	A relation btw $\mathbb{C}$, $\mathbb{R}$ (Definition 5.2)
$L^{\mathbb{A}}$	A relation btw $\mathbb{P}^{\mathbb{A}}$, $\overline{\mathbb{R}}^{\mathbb{A}}$ (Definition 6.1)

4 DESIGN PRINCIPLES

In this section we overview the core PiGen design principles, with the Purchases table of the Introduction used as the running example to explain their impact. Subsequently, in Sections 5 through 8, each principle is described in detail. To set the stage, here are some basic definitions underlying our work.

Definition 4.1. A *block* is a bag of points (i.e. tuples) in the data space $\mathbb{D}$ of the synthetic table $\mathcal{T}$.

Definition 4.2. A *projection block* is a subset of points from $\mathbb{D}^{\mathbb{A}}$, where $\mathbb{D}^{\mathbb{A}}$ represents the data subspace of the synthetic table $\mathcal{T}$ spanned by a given PAS $\mathbb{A}$.

4.1 Region Partitioning

To model the filter predicates associated with $\mathbb{W}$, the data space $\mathbb{D}$ is logically partitioned into a set of blocks. Each block satisfies the condition that every data point in it satisfies the same subset of filter predicates.

The row cardinality of each block is represented using a variable in the LP. The resultant system is usually highly under-determined and therefore, to reduce the complexity of solving it, we leverage the *region partitioning* technique from [23], which partitions the data space into the minimum number of blocks.

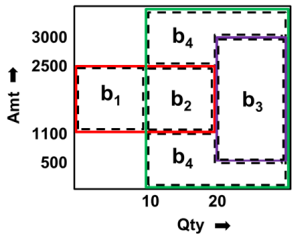

Figure 1: Region Partitioning

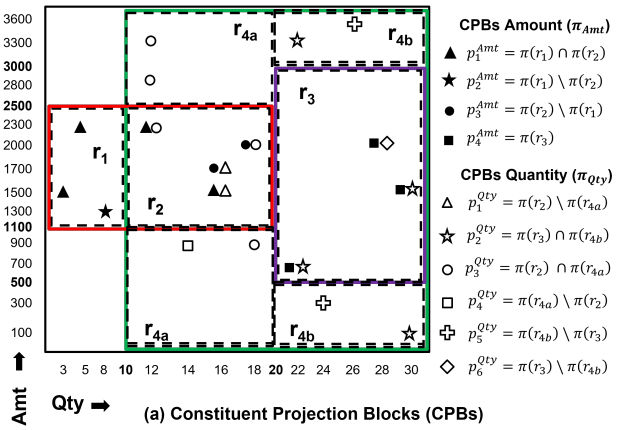

Amt	1500	2300	1300	2300	2000	1700	1500	3300	2800
Qty	3	5	8	12	18	16	16	12	12

Amt	900	900	3300	3600	300	100	700	1500	2000
Qty	14	18	22	26	24	30	22	30	28

(b) Sample Purchases Table (Distinct Rows)

Figure 2: Symmetric Refinement and PSD

Here, for a tuple $t \in \mathbb{D}$, and a PIC $c \in \mathbb{W}$, let $c(t)$ denote the indicator, set to 1 if t satisfies the filter predicate associated with c, 0 otherwise. Now, a pair of tuples t_1 and t_2 are said to be related by $R^{\mathbb{W}}$, if $c(t_1) = c(t_2)$, for all $c \in \mathbb{W}$. $R^{\mathbb{W}}$ is an equivalence relation, and the region partitioning algorithm returns the quotient set of $\mathbb{D}$ by $R^{\mathbb{W}}$. That is, the data points from the same equivalence class (wrt $R^{\mathbb{W}}$) form a block. Each resultant block is referred to as a *filter-block* (FB). The algorithm outputs the domain of each FB, which forms its logical condition. The domain of an FB b is denoted as $D(b)$.

To make the above concrete, consider the three filter predicates, f_1, f_2, f_3 on Purchases. For simplicity, Figure 1 shows only the 2D data space comprising the *Qty* and *Amt* attributes since no conditions exist on the other attributes. In this figure, the filter predicates are represented using regions delineated with colored solid-line boundaries. When region partitioning is applied on this scenario, it produces the four disjoint FBs: b_1, b_2, b_3, b_4, whose domains are depicted with dashed-line boundaries.

4.2 Isolating Projections

To circumvent inter-projection subspace dependencies, we "isolate" the projections. Specifically, a *symmetric refinement* strategy is executed to refine each FB into a set of disjoint blocks, called *refined-blocks* (RBs). The refinement is executed such that each resultant RB exhibits translation symmetry along each applicable projection subspace. That is, for each domain point of an RB r along a particular PAS, the projection of the domain of r along the remaining attributes is identical.

For instance, consider FB b_4 in Figure 1. Clearly, it is asymmetric along the PAS *Qty* – specifically, compare the spatial layout in the range $10 \leq Qty < 20$ with that in $Qty \geq 20$. After refinement, this block breaks into r_{4a} and r_{4b} as shown in Figure 2(a) – it is easy to see that r_{4a} and r_{4b} are symmetric. (The other FBs (b_1, b_2, b_3) happen to be already symmetric, and are shown as r_1, r_2 and r_3, respectively, in Figure 2(a)). This refinement allows for the values along different projection subspaces to be generated independently. That is, $D(r) = D(\pi_{Amt}(r)) \times D(\pi_{Qty}(r))$, for each RB r.

The above refinement, however, does not scale when the projections applied on an FB are along partially overlapping PASs, i.e. when different PASs share some attribute(s). Therefore, to eliminate such situations, we resort to *decomposing* the workload into non-overlapping sub-workloads using a *vertex coloring*-based strategy. As a consequence, for each such sub-workload, a separate summary is produced at the conclusion of the LP solution process.

4.3 Projection Subspace Division

To deal with intra-projection subspace dependencies, the domain of each PAS is logically divided into a set of projection blocks, called *constituent-projection-blocks* (CPBs). This construction ensures that each projection cardinality is expressible as a *summation* over the cardinalities of these CPBs. Further, we ensure that the minimum number of CPBs is produced, aiding in efficient LP formulations.

For our example scenario, PiGen divides the data subspace associated with the *Amt* dimension into 4 CPBs: $p_1^{Amt}, p_2^{Amt}, p_3^{Amt}, p_4^{Amt}$, and the *Qty* dimension subspace into 6 CPBs: $p_1^{Qty}, p_2^{Qty}, ..., p_6^{Qty}$, as shown in Figure 2(a). Each CPB has a semantic meaning associated with it. For example, p_1^{Amt} semantically represents the *Amt* values present in both r_1 and r_2. Further, the CPBs need not be mutually disjoint, as in the case of p_3^{Amt} and p_4^{Amt}. Finally, Figure 2(a) also shows the unique tuples enumerated by the sample output table shown in Figure 2(b), and the CPB (s) to which each of these tuples belongs.

4.4 Constraints Formulation

The LP solving procedure is constructed using variables representing the row cardinalities of RBs and CPBs. For instance, if x_i represents the cardinality of RB r_i, and y_j^{Amt} and y_k^{Qty} represent

the cardinalities of CPBs p_j^{Amt} and p_k^{Qty}, respectively, then PICs are expressed by linear equations as follows:

$$c_1: \quad x_1 + x_2 = 500, \quad y_1^{Amt} + y_2^{Amt} + y_3^{Amt} = 5$$
$$c_2: \quad x_3 = 1000, \quad y_4^{Amt} = 3$$
$$c_3: \quad x_2 + x_3 + x_{4a} + x_{4b} = 3000,$$
$$y_1^{Qty} + y_2^{Qty} + y_3^{Qty} + y_4^{Qty} + y_5^{Qty} + y_6^{Qty} = 9$$

Finally, additional sanity constraints are added to the LP to ensure data constructibility. For example, the distinct row-cardinality of the projection of an RB is upper-bounded by the RB's native cardinality.

4.5 Enriched Database Summary

To construct the final summary, the domain of each PAS is divided into a set of intervals and then the CPBs are assigned these intervals. A sample summary for the Purchases table is shown in Figure 3, after incorporating an additional attribute *Year* to illustrate a multi-dimensional projection.

Each segment of the summary corresponds to a populated RB. Specifically, the figure shows the tabulation for the r_1, r_3 and r_{4b} RBs. Each tabulation comprises of a column for each PAS acting on the RB, and an additional last column indicating the total number of tuples present in the RB. In each PAS column, the information for generating data of the associated projection subspace is present. Specifically, we maintain the intervals in the projection subspace along with their distinct counts. As a case in point, the first tabulation, corresponding to r_1, is interpreted as "generate 500 tuples, such that there are 5 distinct values of *Amt* in the interval `[1100,2500)`, and 20 distinct value pairs of {*Qty*, *Year*} of which 12 are from the 2D interval `[1,10), [1990,2000)`, and the remaining 8 from the 2D interval `[1,10), [2010,2020)`."

r_1

Amt	Qty, Year	#Tuples
[1100, 2500): 5	(Q) [1, 10), (Y) [1990, 2000): 12 (Q) [1, 10), (Y) [2010, 2020): 08	500

r_3

Amt	Qty	Year	#Tuples
[500, 3000): 3	[20, 25): 5 [25, 40): 4	[1990,2020)	1000

r_{4b}

Qty	Amt, Year	#Tuples
[20, 25): 5	(A) [1,500) U [3000,3600), (Y) [1990, 2020): 6	2000

Figure 3: PiGen Table Summary

For attributes that do not feature in any projection subspace, no associated distinct cardinality is maintained – an example is *Year* in r_3. Lastly, the primary-key column (*PID* in the example) is omitted from the summary and is assumed to be a sequence of distinct natural numbers during on-demand tuple generation.

In the following sections, we present the internal details of each of the aforementioned concepts.

5 ISOLATING PROJECTIONS

To facilitate independent processing of projection sub-spaces, we refine the FBs so that the resultant blocks become symmetric. The symmetry is formally defined as follows:

Definition 5.1. A block r in the data space of a $\mathbb{U}$-dimensional table $\mathcal{T}$ is symmetric along a PAS $\mathbb{A}$ iff

$$D(r) = D(\pi_{\mathbb{A}}(r)) \times D(\pi_{\mathbb{U}\setminus\mathbb{A}}(r))$$

where $D(.)$ returns the domain of the input block.

Likewise r is symmetric along PASs $\mathbb{A}_1, \mathbb{A}_2, ..., \mathbb{A}_\alpha$ iff

$$D(r) = D(\pi_{\mathbb{A}_1}(r)) \times D(\pi_{\mathbb{A}_2}(r)) \times ... \times D(\pi_{\mathbb{A}_\alpha}(r)) \times D(\pi_{\mathbb{U}\setminus(\mathbb{A}_1\cup\mathbb{A}_2\cup...\cup\mathbb{A}_\alpha)}(r))$$

The Cartesian product implies that for a symmetric block, the data can be *independently* generated for each PAS considered. Therefore, Symmetric Refinement module refines each FB into a set of symmetric blocks along the PASs acting on it. Hence, post-refinement, the different projection spaces can be processed independently. The refinement algorithm is discussed in Section 5.1.

Impact of Overlapping Projection Subspaces. When partially overlapping PASs, say $\mathbb{A}_1$ and $\mathbb{A}_2$, are applied on an FB b, symmetric refinement becomes computationally challenging. This is because $\mathbb{A}_1, \mathbb{A}_2$ have to be made conditionally independent for b, requiring refinement such that each resulting block is symmetric along $\mathbb{A}_1$ and $\mathbb{A}_2$ for *each* domain point in $D(\mathbb{A}_1 \cap \mathbb{A}_2)$. This is easily done by enumeration for small cardinality domains, but does not scale in general. Hence, in PiGen we bypass such overlapping projection operations by ensuring, as described in Section 5.2, that the input workload is initially itself decomposed such that there are no projection subspace overlaps in the resulting sub-workloads.

5.1 Symmetric Refinement

The refinement for each FB is done independently. Given an FB b and its associated PASs, this module refines b into a group of RBs, such that each RB is symmetric along the input PASs.

Let us first understand the refinement procedure along a single PAS $\mathbb{A}$. Here, given b and $\mathbb{A}$, the refinement is carried out as follows:

(1) Let $\mathbb{I}$ be the subset of all interval-combinations in $D(\mathbb{A})$ that are present in b. The interval boundaries along an attribute are computed using the constants that appear in the filter predicates of the input PICs. For some interval-combination $\mathcal{I} \in \mathbb{I}$, let $b_{\mathcal{I}}$ denote the part of b whose projection along $\mathbb{A}$ is $\mathcal{I}$.
(2) For each interval combination $\mathcal{I} \in \mathbb{I}$, the projection of $b_{\mathcal{I}}$ along $\mathbb{U} \setminus \mathbb{A}$ is computed, and denoted as $\pi(b_{\mathcal{I}})$.
(3) A hashmap H is created with keys as $\pi(b_{\mathcal{I}})$ and value as $\mathcal{I}$. Hence, the parts of b where the projection of b along $\mathbb{U} \setminus \mathbb{A}$ do not alter with changing values of $\mathbb{A}$ are clubbed together into a single hash entry. This construction provides independence between $\mathbb{A}$ and the $\mathbb{U} \setminus \mathbb{A}$ subspaces.
(4) Each entry e in H corresponds to an RB, constructed by taking the region stored as key in e for the $\mathbb{U} \setminus \mathbb{A}$ attribute-set, and a union of regions stored as value in e for the $\mathbb{A}$ attribute-set.

Interestingly, the above refinement strategy also ensures that the number of resultant blocks is kept to a *minimum*, as proved in [21].

Extension to Multiple PAS. We now move on to the multiple PAS scenario. Let there be α PASs $(\mathbb{A}_1, \mathbb{A}_2, ..., \mathbb{A}_\alpha)$ applicable on b across all PICs. This implies that there are $\alpha + 1$ projection subspaces –

$\pi_{\mathbb{A}_1}(b)$, $\pi_{\mathbb{A}_2}(b)$, ..., $\pi_{\mathbb{A}_\alpha}(b)$, and $\pi_{\mathbb{U}\setminus(\mathbb{A}_1\cup\mathbb{A}_2\cup\ldots\cup\mathbb{A}_\alpha)}(b)$. It is easy to see that the block becomes symmetric when refined along any α of these $\alpha + 1$ subspaces.

The refinement is done iteratively, where the output of refinement along one subspace is fed into the next in the sequence. Since any sequence among the chosen α subspaces results in a symmetric block, there are a total of $\binom{\alpha+1}{\alpha}\alpha!$ ways to do the refinement. The specific choice that we make from this large set of options is important because it has an impact on the number of variables in the LP, and hence the computational complexity and scalability of the solution procedure. In particular, the number of CPBs created depends on the geometry of the RBs, and usually more overlaps of RBs along a PAS results in more CPBs. More precisely, if we refine a block along a subspace, the overlaps in that space remain unaffected, but the overlaps along the *remaining subspaces* may increase. Therefore, to minimize this collateral impact, we adopt the following greedy heuristic in PiGen: The subspace having the maximum FB overlaps with b is chosen as the next subspace to be refined in the iterative sequence.

Mapping RBs to PICs. The set of RBs, denoted by $\mathbb{R}$, are connected with the set of PICs using the following relation:

Definition 5.2. An RB $r \in \mathbb{R}$ is related by relation M to a PIC c containing filter predicate f, iff $D(r)$ satisfies f. That is,

$$rMc \Leftrightarrow t \text{ satisfies } f, \forall t \in D(r)$$

For a PIC c, the associated filter predicate's output cardinality l can be expressed as the union of a group of RBs related to c by M, as follows:

$$|\bigcup_{r:rMc} r| = \sum_{r:rMc} |r| = l$$

Since all the RBs are mutually disjoint, the union could be replaced with summation in the above equation.

5.2 Workload Decomposition

As discussed previously, symmetric refinement is performed when distinct PASs applicable on an FB are non-overlapping. This holds true when, for each domain point t, the distinct PASs across various PICs that are applicable on t, are mutually disjoint. For any given collection of sets (PASs) to be mutually disjoint, it is equivalent to say that they are *pairwise disjoint*. This leads us to defining the concept of an *intersecting pair* of PICs.

Definition 5.3. A pair of PICs ($c_1 : \langle f_1, \mathbb{A}_1, l_1, k_1\rangle$, $c_2 : \langle f_2, \mathbb{A}_2, l_2, k_2\rangle$) intersect iff:

- their PASs partially intersect, i.e.,

$$\mathbb{A}_1 \cap \mathbb{A}_2 \neq \emptyset, \mathbb{A}_1 \neq \mathbb{A}_2, \text{ and}$$

- f_1 and f_2 overlap, i.e., there exists a point t in the domain space of $\mathcal{T}$ such that t satisfies f_1 and f_2.

For example, consider the following pair of constraints, c_4 and c_5, on the Purchases table:

$$c_4 : \langle Amt \leq 2500 \wedge Year \geq 1990, (Qty, Year), 500, 20\rangle$$

$$c_5 : \langle Qty \geq 20 \wedge Year \leq 2020, (Amt, Year), 2000, 6\rangle$$

We see that the filters in the two constraints overlap, and the corresponding PASs also partially intersect.

In the Workload Decomposition module, the input workload is split such that there are no intersecting pairs of PICs in the resulting sub-workloads. We refer to a workload with no intersecting pairs as a *compatible* workload, and denote it using $\mathbb{C}$.

Given an original workload $\mathbb{W}$, the set of intersecting pairs IP is computed first. Subsequently, we construct compatible sub-workloads $\mathbb{C}_1, \mathbb{C}_2, .., \mathbb{C}_n$ that cover the entire workload. Additionally, we aim towards minimizing n, i.e. the number of sub-workloads. This minimization is desirable to facilitate common platform for workload performance evaluation. Since the minimization is NP-complete (reduction from vertex coloring), we adopt a heuristic based on greedy vertex coloring. The algorithm iterates over the PICs, and in each iteration, the PIC c with minimum intersections in IP is picked and assigned to a compatible sub-workload $\mathbb{C}_i$. If multiple compatible options are available, an assignment that minimizes the skew in the sub-workload sizes is made. On the other hand, if no such assignment is possible, a new sub-workload is constructed, and initialized with c.

In the worst case, the above algorithm can create one sub-workload per query. However, it is our experience that in practice, a small number of sub-workloads is usually sufficient. Further, we hasten to add that even if the worst case materializes, the overheads incurred would be marginal as only a single small summarized table is stored per sub-workload.

6 PROJECTION SUBSPACE DIVISION

We now turn our attention to handling intra-projection subspace dependencies. The projection output cardinality with respect to a PIC c can be expressed using the relation M as follows:

$$|\bigcup_{r:rMc} \pi_{\mathbb{A}}(r)| = k$$

We use the shorthand $\bar{r}$ to represent the projection of an RB r on $\mathbb{A}$, i.e. $\bar{r} = \pi_{\mathbb{A}}(r)$, and this projection block is referred to as a *projected-refined-block* (PRB). The set of all PRBs for a PAS $\mathbb{A}$ is shown as $\overline{\mathbb{R}}^{\mathbb{A}}$. Further, for brevity, we overload the same relation M to establish an association between PRB $\bar{r}$ and a constraint c. That is, $\bar{r}Mc \Leftrightarrow rMc$. Hence we can rewrite the above equation as:

$$|\bigcup_{\bar{r}:\bar{r}Mc} \bar{r}| = k$$

The union here cannot be replaced with summation because unlike RBs, the PRBs need not be disjoint. Therefore, to be able to express the constraint as a linear equation, the projection subspace $\mathbb{D}^{\mathbb{A}}$ needs to be divided into a set of CPBs. The set of CPBs corresponding to a PAS $\mathbb{A}$ is denoted using $\mathbb{P}^{\mathbb{A}}$. Each element $p \in \mathbb{P}^{\mathbb{A}}$ logically represents a subset of $\mathbb{D}^{\mathbb{A}}$. Further, a relation $L^{\mathbb{A}}$ is provided that connects the elements of $\mathbb{P}^{\mathbb{A}}$ with elements of $\overline{\mathbb{R}}^{\mathbb{A}}$. We first define the notion of what constitutes a valid division, and then go on to presenting an algorithm that provides the (unique) optimal division.

6.1 Valid Division

A valid division is defined as follows:

Definition 6.1. Given $\mathbb{C}, \overline{\mathbb{R}}^{\mathbb{A}}$ and M, a division $(\mathbb{P}^{\mathbb{A}}, L^{\mathbb{A}})$ with respect to a projection data subspace $\mathbb{D}^{\mathbb{A}}$ is called a *valid division* if it satisfies the following two conditions:

Condition 1. Each PRB $\overline{r} \in \overline{\mathbb{R}}^{\mathbb{A}}$ is expressible as a union of a group of elements from $\mathbb{P}^{\mathbb{A}}$, determined by relation $L^{\mathbb{A}}$:

$$\overline{r} = \bigcup_{p:pL^{\mathbb{A}}\overline{r}} p, \quad \forall\, \overline{r} \in \overline{\mathbb{R}}^{\mathbb{A}}$$

Condition 2. All elements in $\mathbb{P}^{\mathbb{A}}$ that are related to a constraint $c \in \mathbb{C}$ through the composite relation

$$M \circ L^{\mathbb{A}} = \{(p, c) | \exists \overline{r} \in \overline{\mathbb{R}}^{\mathbb{A}} : \overline{r} M c \wedge p L^{\mathbb{A}} \overline{r}\}$$

(i.e., all elements of the set $\{p : (p, c) \in M \circ L^{\mathbb{A}}\}$), should be *mutually disjoint* for all $c \in \mathbb{C}$.

Condition 1 is needed to associate a PRB with its constituent CPBs. This is required during data generation in order to populate appropriate RBs based on the cardinalities of CPBs obtained from the LP solution. Condition 2 enforces that each constraint is comprised of disjoint constituent CPBs, thereby enabling expression of the constraints as linear equations.

For ease of presentation, we drop $\mathbb{A}$, which can be assumed implicitly, from the superscript in the rest of this section.

6.2 Optimal Division

The number of CPBs in $\mathbb{P}$ determine the number of variables in the LP. Therefore, reducing the size of $\mathbb{P}$ helps in reducing the LP complexity, providing workload scalability and computational efficiency. Hence, we define an *optimal division* as a valid division that has the minimum number of CPBs.

Definition 6.2. A valid division $(\mathbb{P}, L)$ is called an optimal division iff there does not exist any other valid division $(\mathbb{P}', L')$ such that $|\mathbb{P}'| < |\mathbb{P}|$. We represent the optimal division by $(\mathbb{P}^*, L^*)$.

Each element p of $\mathbb{P}$ maps to a collection of sets from $\overline{\mathbb{R}}$ using L. Let $\overline{\mathbb{R}}(p)$ represent the set of PRBs that are related to p through L. Therefore, as a first step towards identifying the optimal division, let us characterize how CPBs interact with PRBs as follows: Consider a vector v_p corresponding to each CPB p in $\mathbb{P}$. The vector is of length m, where each element is associated with an element of $\overline{\mathbb{R}}$. Further, the element associated with $\overline{r} \in \overline{\mathbb{R}}$ is denoted by $v_p(\overline{r})$. Specifically, element $v_p(\overline{r})$ is set to 1 iff $pL\overline{r}$. For such cases, $p \subseteq \overline{r}$. Next, the elements in v_p corresponding to the sets $\overline{\mathbb{R}}(p') \setminus \overline{\mathbb{R}}(p)$ for all p' such that $(p, c), (p', c) \in M \circ L$ for some $c \in \mathbb{C}$, are represented as 0, denoting the absence of values from these sets (using Condition 2). The remaining elements of v_p are set as '$\times$' denoting a *don't care* state, i.e. p and $\overline{r}$ may or may not have an intersection. Finally, p can be expressed in terms of v_p as:

$$p = \bigcap_{\overline{r}:v_p(\overline{r})=1} \overline{r} \setminus \bigcup_{\overline{r}':v_p(\overline{r}')=0} \overline{r}' \tag{1}$$

Let the set of vectors corresponding to the elements in $\mathbb{P}^*$ be denoted as $\mathbb{V}^*$ – the algorithm for computing this set is given below.

Opt-PSD Algorithm. We begin our computation of the projection subspace division by creating a *Division Graph*. In this graph, a vertex is created corresponding to each element of $\overline{\mathbb{R}}$. Then, an edge is added between vertices corresponding to $\overline{r}_1$ and $\overline{r}_2$ if there exists a constraint c such that $\overline{r}_1 M c$ and $\overline{r}_2 M c$, (i.e. both PRBs are related to a common constraint c), and the domains of $\overline{r}_1$ and $\overline{r}_2$ intersect. The resultant graph G is given as input to Algorithm 1, which returns the set of vectors $\mathbb{V}^*$ in the output. Leveraging the vectors, the contents of the CPBs are computed using Equation 1. Then, the L^* relation is populated with the expression: $(p, \overline{r}) \in L^*$, if $v_p(\overline{r}) = 1, v_p \in \mathbb{V}^*$. The rest of the algorithm proceeds as follows:

Algorithm 1: Optimal Projection Subspace Division

```
Input: Division Graph G
Output: Optimal Vectors-set V*
1  toBeSplit ← ∅;
2  for r̄ in R̄ do
3      v_init ← {×}^m, v_init(r̄) ← 1;
4      toBeSplit ← {v_init};
5      while toBeSplit ≠ ∅ do
6          v ← toBeSplit.pop();
7          pivot, targets ← getPivot(G, v);
8          if pivot exists then
9              toBeSplit ← toBeSplit ∪ Split(v, targets);
10         else
11             V* ← V* ∪ {v};
12 return V*;
```

Firstly, we iterate over the vertices of G. In the iteration for a PRB $\overline{r}$, a vector is initialized with '$\times$' for all the positions except that corresponding to $\overline{r}$, which is set to 1 (Line 3 of Algorithm 1). These initial vectors are recursively further split in the while loop (Line 5), using a running list of vectors called *toBeSplit*.

Secondly, in each iteration of the while loop, an element v from *toBeSplit* is popped and split using a *pivot* vertex; the resultant elements are re-inserted in the list. A pivot PRB is distinguished as one which is included in v and co-occurs in a constraint c with another PRB (target) whose current assignment in the vector is $\times$. To select the *pivot* vertex in G, the *getPivot* function is used, which makes the choice based on the following conditions: (a) $v(pivot) = 1$, and (b) there exists a PRB $\overline{r}$ such that there is an edge between the vertices corresponding to *pivot* and $\overline{r}$. Further, the value for $\overline{r}$ in the vector v is $\times$.

Finally, the collection of all PRBs that satisfy condition (b) is denoted as the *targets* set corresponding to *pivot*, and is returned by the *getPivot* function. Now, v is split using the *Split* function (detailed in [21]), which computes a powerset enumeration of the vector positions corresponding to PRBs in *targets*.

We have also incorporated optimizations to Algorithm 1 to prevent redundant computations. Due to space limitations, these optimizations, along with the algorithm's proof of correctness and optimality, are deferred to [21].

7 CONSTRAINTS FORMULATION

LP formulation requires constraints that capture the PICs while ensuring that the solution corresponds to a physically constructible database. In a valid division, each PRB is covered by a set of CPBs and all CPBs related to a same PIC are mutually disjoint. As a consequence, a constraint $c\ \langle f, \mathbb{A}, l, k\rangle$ can now be expressed as a summation of cardinalities of CPBs related to c through $M \circ L^{\mathbb{A}}$:

$$|\pi_{\mathbb{A}}(\sigma_f(\mathcal{T}))| = \sum_{p:(p,c)\in M\circ L^{\mathbb{A}}} |p| \tag{2}$$

Further, since each $\overline{r} \in \overline{\mathbb{R}}^{\mathbb{A}}$ is related to at least one $c \in \mathbb{C}$ through $M \circ L^{\mathbb{A}}$, the CPBs associated with $\overline{r} \in \overline{\mathbb{R}}^{\mathbb{A}}$ through $L^{\mathbb{A}}$ are also disjoint. Hence, the cardinality of $\overline{r} \in \overline{\mathbb{R}}^{\mathbb{A}}$ can be represented as a summation of the cardinalities of related CPBs:

$$|\overline{r}| = \sum_{p:pL^{\mathbb{A}}\overline{r}} |p| \tag{3}$$

The LP construction uses the above facts while constructing constraints. Specifically, two types of LP variables are constructed – x_r and y_p, denoting $|r|$ ($r \in \mathbb{R}$) and $|p|$ ($p \in \mathbb{P}^{\mathbb{A}}$), respectively.

Given this framework, there are two classes of constraints, *Explicit Constraints* and *Sanity Constraints*, that constitute the input to the LP and are discussed in the remainder of this section.

7.1 Explicit Constraints

These are the LP constraints that are directly derived from the PICs. Specifically, for each PIC, $c : \langle f, \mathbb{A}, l, k \rangle$, the following pair of constraints is added for Filter and Projection Output:

(a) Filter Output	**(b) Projection Output** (from Equation 2)
$\sum_{r:rMc} x_r = l$	$\sum_{p:(p,c)\in M\circ L^{\mathbb{A}}} y_p = k$

7.2 Sanity Constraints

These are the additional constraints necessary and sufficient to ensure that the LP solution can be used for constructing a physical database instance. Here, there are three types of constraints:

Type 1: These constraints ensure that the row cardinality for each RB and CPB are non-negative in the LP solution. That is,

$$x_r \geq 0, \forall r \in \mathbb{R}, \quad \text{and} \quad y_p \geq 0, \forall p \in \mathbb{P}^{\mathbb{A}}, \text{ for all PAS } \mathbb{A}$$

Type 2: These constraints ensure the row cardinality for each RB is $\geq$ the number of distinct tuples along each applicable PAS for it. Using Equation 3, these constraints, for each RB r and each of its associated PAS $\mathbb{A}$, are expressed as:

$$\sum_{p:pL^{\mathbb{A}}\overline{r}} y_p \leq x_r$$

Type 3: Even after satisfying the above sanity constraints, the total number of tuples for an RB may be positive while the number of distinct tuples along some projection subspace remains 0. This possibility is prevented by the following constraint for each RB r and each associated PAS $\mathbb{A}$:

$$x_r \leq |\mathcal{T}| \sum_{p:pL^{\mathbb{A}}\overline{r}} y_p$$

In the above, $\overline{r} = \pi_{\mathbb{A}}(r)$ and $|\mathcal{T}|$ is the cardinality of $\mathcal{T}$, which is an upperbound on x_r. We assume that $|\mathcal{T}|$ is given as an input PIC with no filter predicate.

8 DATA GENERATION

The table summary compactly stores information needed for generating the associated tuples. In this section, we first discuss how the summary is constructed and then the tuple generation process.

8.1 Summary Construction

Each projection subspace is dealt with independently thanks to the projection isolation techniques. Consider the projection subspace corresponding to PAS $\mathbb{A}$ – here, the first step is to assign an interval to each CPB $p \in \mathbb{P}^{\mathbb{A}}$. A challenge in this assignment is that the domains of different CPBs may intersect. For instance, the domains of CPBs p_2^{Qty} and p_6^{Qty} intersect in Purchases. However, since CPBs related to a common projection constraint should not intersect, we assign disjoint intervals to these CPBs to ensure Condition 2. Hence, p_2^{Qty} and p_6^{Qty} are allocated disjoint intervals for PAS Qty as $(p_2^{Qty}, c_3), (p_6^{Qty}, c_3) \in M \circ L^{Qty}$. On the other hand, in the case of PAS Amt, p_2^{Amt} and p_4^{Amt} are not related to any c in $\mathbb{C}$, and therefore their data generation intervals can overlap.

As per above, a feasible interval assignment for Purchases is:

$p_2^{Amt} \leftarrow [1100, 2500)$	$p_2^{Qty} \leftarrow [20, 25)$
$p_4^{Amt} \leftarrow [500, 3000)$	$p_6^{Qty} \leftarrow [25, 40)$

The summary is maintained RB-wise, with the template structure shown in Figure 4. We see here that all the CPBs associated with the block, along with their distinct tuple cardinalities, are represented in the summary. Using α to denote the total number of associated PASs, an RB can be represented in $\alpha + 1$ components, with each component associated with a PAS having a distinct row-cardinality. For the attribute-set on which no projection is applied for the RB, shown as $\mathbb{A}_{left}$, the domain of the projection block is kept as is and no distinct tuple count is maintained. Lastly, each RB has an associated total cardinality. A populated instance of the template, and its interpretation, was discussed earlier in Section 4.5.

$\mathbb{A}_1$	$\mathbb{A}_2$	...	$\mathbb{A}_\alpha$	$\mathbb{A}_{left}$	
CPB_1: card.,	CPB_1: card.,	...	CPB_1: card.,		RB
CPB_2: card.,	CPB_2: card.,	...	CPB_2: card.,	PB	Card.
...	...	...	...		

Figure 4: Sample RB in Summary

8.2 Tuple Generation

Using the information in the summary, the tuples of the table are instantiated. Specifically, the algorithm iterates over each RB and generates the number of rows specified in the associated total cardinality value. For an RB and an associated PAS $\mathbb{A}$, each CPB is picked and the corresponding partial tuples are generated. This gives a collection of partial tuples for $\mathbb{A}$ which may be less than the total cardinality. To make up the shortfall without altering the number of distinct values, we repeat the generated partial tuples until the total cardinality is reached. For the $\mathbb{A}_{left}$ component, which only has a single interval, any partial-tuple within its boundaries can be picked for repetition. Finally, partial-tuples across all projection spaces of the RB are concatenated to construct its output tuples.

Inter-Block Dependencies. We have to ensure that the partial-tuples associated with a CPB are identical for each of the associated RBs. To do so, we employ a deterministic algorithm that takes an interval and a cardinality as input, and produces a series of distinct points, equal to the cardinality, from the interval – this series is used in all the associated RBs. As a case in point, for the sample summary in Figure 3, the partial tuples generated for the CPB with interval $[20, 25)$ and distinct row cardinality 5 are identical in both r_3 and r_{4b}.

9 PIGEN DEPLOYMENT

The end-to-end data generation pipeline starts with a workload $\mathbb{W}$ of PICs over a table $\mathcal{T}$ serving as the pipeline input. Then **Workload Decomposition** splits $\mathbb{W}$ into a set of compatible sub-workloads. Subsequently, the rest of the pipeline, comprising of LP Formulation and Data Generation, is executed independently for each of these sub-workloads. The **LP Formulation** for a sub-workload $\mathbb{C}$ begins with **Region Partitioning** followed by **Symmetric Refinement** algorithm. This gives the set of RBs. For each PAS across all PICs, the PRBs are computed using the RBs. These PRBs and $\mathbb{C}$ are then used by the **Projection Subspace Division** module to construct the set of CPBs. Next, at the **Constraints Formulation** stage, an LP is constructed using variables representing the cardinalities of RBs and CPBs. This construction is then given as the input to the **LP Solver**. From the solution produced by the LP solver, a comprehensive table summary is constructed using the **Summary Construction** module. This summary is used by the **Tuple Generation** module to synthesize the data. It can generate tuples on-demand during query processing, thereby eschewing the need for data materialization. Alternatively, if the user desires a materialized database instance, it can be generated from the summary and stored persistently.

Finally, PiGen leverages the graphical model-based table decomposition techniques proposed in [8] to construct the table in a piece-meal fashion and then stitch these constituent pieces together. Each sub-table consists of a subset of attributes determined by the attributes that co-appear in the PICs, thereby further reducing the LP complexity.

Having presented the mechanics of PiGen, we now take a step back and critique the approach on relevant aspects.

9.1 Workload Feasibility

Feasibility of a set of PICs implies that the PICs can be accurately satisfied by a single database instance. This notion can be classified into the following two scenarios:

Intra-PIC Feasibility. This form of feasibility deals with PICs at an individual level. Specifically, a PIC $c : \langle f, \mathbb{A}, l, k\rangle$ is feasible iff:

$$0 < k \leq l \leq |\mathcal{T}| \text{ or } l = k = 0 \tag{4}$$

We prove this in the full version of the paper [21].

Inter-PIC Feasibility. This is a stronger form of feasibility, where in addition to PICs being individually feasible, they are also required to be mutually compatible. For instance, consider the additional constraint, c_6, on the Purchases table:

$$c_6 : \langle Amt \leq 2000 \wedge Year \geq 2000, Qty, 400, 25\rangle$$

We observe here that c_4 and c_6 cannot be satisfied together. Specifically, c_6 requires 25 distinct Qty values for the range $Amt \leq 2000 \wedge Year \geq 2000$, while c_4 requires that the number of distinct $(Qty, Year)$ pairs is 20 for a larger covering range, constituting an impossible situation.

Defining a set of necessary and sufficient conditions that ensure solution feasibility for various types of input constraints has been looked at in the database literature. For instance, [17] deals with *schematic* constraints on the participation cardinalities for the relationships between entities in the ER model, and provides necessary and sufficient conditions to determine whether database instances exist such that all entities and relationships are populated. However, giving a similar holistic solution in the *statistical* query-based constraints space, is still an open problem, although restricted versions have been attempted. Specifically, feasibility of projection cardinality constraints has been discussed in [12, 16, 27]. A class of constraints, called **BT** inequalities, were proposed in [12], which capture the necessary conditions to be satisfied by the projection output cardinalities. However, this constraint set is not sufficient, making it still possible that no actual database can satisfy these values. Subsequently, another class of constraints, called **NC** (non-uniform cover) inequalities, was proposed in [27]. While this constraint set creates sufficient conditions for database construction, the limitation is that satisfiability of these conditions is not guaranteed. Further, the feasibility space does not exhibit a convex behaviour, making it inexpressible as a set of linear constraints [16].

9.2 Solution Guarantees

We discuss the solution guarantees for feasible and infeasible workloads separately below.

Feasible Workload. The input workload feasibility is true by definition when the PICs have been derived from an existing setup. In such scenarios, PiGen ensures, thanks to the explicit LP constraints, that the generated data satisfies the PICs with 100% accuracy. Further, the sanity constraints ensure the LP solution is always constructible. This leads us to the following lemma:

Lemma 9.1. *For a feasible and compatible set of PICs, PiGen always produces an instance of the table that satisfies all the constraints.*

Given an initially feasible workload, workload-decomposition can always produce sub-workloads that are both feasible and compatible. Therefore, for any initially feasible workload, the data produced by PiGen can cover all the input constraints. We formally prove Lemma 9.1 in Appendix A.

Infeasible Workload. Intra-PIC feasibility check can be trivially verified at the pre-processing stage by checking the adherence of constraints to Condition 4. However, if the input has inter-PIC infeasibility, the following two possibilities may arise: (a) It may so happen that Workload Decomposition, while resolving intersection PICs, may as a *collateral benefit*, also produce feasible sub-workloads. For example, by partitioning the workload $\{c_4, c_5, c_6\}$ into $\{c_4\}$ and $\{c_5, c_6\}$, the resulting sub-workloads become non-intersecting as well as feasible. In this scenario, PiGen produces one table for each sub-workload (using Lemma 9.1). (b) Alternatively, in case this beneficial effect of decomposition does not happen, then the LP constraints (discussed in Section 7) themselves become infeasible. Hence, the LP solver eventually flags this infeasibility. We have explicitly verified this to be the case for the Z3 solver with a few deliberately created infeasible constraint sets.

9.3 Solution Complexity

Computationally, the bottleneck of the pipeline lies in the LP solver. The LP complexity is primarily governed by the number of CPBs created, which is determined by the overlaps between the blocks intra-projection subspaces. The extent of overlaps is reflected by

the outdegree of vertices in the Division Graph $G(V, E)$ introduced in Section 6. For adversarial cases, the number of CPBs can be as high as the number of connected induced subgraphs of G, which can go up to $2^{|V|}$ [21]. Further, $|V|$ itself is $O(2^{|\mathbb{W}|})$. However, these worst-case exponential scenarios are relatively rare in practice, and our experience is that the count is usually well within the solver's computational limits. We quantitatively assess this aspect in our experimental evaluation (Section 10).

Further, for infeasible workloads, the only additional overheads incurred are the checks for intra-PIC feasibility. This verification takes constant time for an input PIC.

Lastly, the decision version of the general data generation problem is `NEXP-complete`, as shown in [8].

9.4 Limitations and Extensibility

While PiGen takes a substantive step towards addressing the primary challenges of projection modeling, there are some practical limitations wrt its current coverage and scope, as described next.

Multiple Summaries. We would ideally like to produce a single summary instance that satisfies all the PICs. However, PiGen may have to produce multiple summaries, and hence multiple databases, to cater to constraint workloads that feature overlapping projection spaces. From a practical perspective, this multiplicity does not impose a substantive overhead due to the minuscule size of each summary. Further, PiGen attempts to reduce the number of sub-workloads to the minimum required to ensure compatibility.

Workload Scale. PiGen currently handles workloads of reasonable complexity as showcased in our experiments. However, for more complex scenarios, a promising recourse is to introduce *approximation*, where volumetric accuracy is marginally compromised to achieve solution tractability. For example, a plausible heuristic could be to not create all the CPBs in one go, but to create them greedily until the error limit is reached. Being a highly underdetermined system, there always exist a sparse solution to the LP – therefore, this iterative process is expected to converge quickly.

Incremental Workloads. Currently the entire constraint workload is assumed to be given as the input. An alternative scenario is where the constraints are incrementally provided. This may appear problematic since PiGen does not allow modifying the solution to satisfy additional constraints. However, its data-scale-free summary creation permits rebuilding the solution from scratch cheaply.

10 EXPERIMENTS

In this section, we evaluate the empirical performance of a Java-based implementation of PiGen. The popular Z3 solver [6] is invoked by the tool to compute the solutions for the LP formulations. Our experiments cover the accuracy, time and space overheads and scalability aspects of PiGen, and are conducted using the PostgreSQL v9.6 engine [3] on a vanilla HP Z440 workstation.

Workload Construction. In presenting the experimental results, we initially focus on fully compatible workloads. Subsequently, in Section 10.5, we discuss the corresponding performance for workloads featuring intersection. A variety of real world and synthetic benchmarks were used in designing the workloads. For representative large fact tables from each of the benchmarks, a workload of compatible PICs was derived by executing a set of queries. The denormalized versions of these tables were considered for constructing PICs. The details of the compatible workloads are as follows:

TPC-DS Suite: This suite comprises of four workloads, corresponding to the four TPC-DS tables [4] subject to the maximum number of projection operations in the benchmark – namely, STORE_SALES (SS), CATALOG_SALES (CS), WEB_SALES (WS), and INVENTORY (INV).

Census Workload: Here, the **Census** dataset framework used in [14] is extended to additionally feature projections apart from the extant filter cardinality constraints. In particular, a single workload was constructed on the PERSONS (P) table.

IMDB Suite: This suite is designed from the JOB [2] benchmark based on the **IMDB** dataset. It comprises of three workloads, corresponding to the three tables subject to the maximum projection operations – namely, MOVIE_KEYWORD (MK), CAST_INFO (CI), and MOVIE_COMPANIES (MC).

The complexity of these various workloads is quantitatively characterized in Table 3. Note that they feature a substantial degree of both inter-projection complexity (up to 10 projection subspaces and 6 dimension subspaces) and intra-projection complexity (maximum degree of the Division Graph vertices goes as high as 72).

Table 3: Workload Complexity

Dataset	Table	# PICs	# PASs	PAS Length		Vertex Degree	
				Avg.	Max.	Avg.	Max.
TPC-DS	SS	16	8	1.4	5	3.95	10
	CS	15	10	2.2	5	4.74	15
	WS	16	8	2	6	5.7	16
	INV	6	3	1.5	4	0.92	4
Census	P	220	3	1.67	2	1.33	72
IMDB	MK	16	4	1.25	2	5.68	14
	CI	14	3	2.67	3	3.7	17
	MC	19	4	1.5	2	3.75	15

Baselines. We compare PiGen against the **DataSynth** and **Hydra** frameworks which both support strict cardinality constraints. For DataSynth, projection constraints need to be restricted to single attribute tables, whereas in Hydra, only the filter constraints are considered in the generation process. We deliberately omit the evaluation of systems dealing with parameterized cardinality constraints such as Touchstone [18] and MyBenchmark [19]). This is due to the organic differences, highlighted in Section 2 between their problem framework and ours, which render quantitative comparisons to be infructuous.

10.1 Constraint Accuracy

When PiGen was run on the aforementioned workloads, the generated data satisfied all the constraints with **100% accuracy**. To appreciate the complexity present in these successfully modeled constraints, we present a representative sample constraint applied on the denormalized relation of STORE_SALES from TPC-DS below:

$$\mathbf{c} : \langle \mathbf{f}, \mathbb{A}, \mathbf{31921358}, \mathbf{15061} \rangle$$

$\mathbf{f}$: $d\_year = 2002 \wedge$
$(i\_category \in (\text{'Jewelry'},\text{'Women'}) \wedge i\_class \in (\text{'mens watch'},\text{'dresses'})) \vee$
$(i\_category \in (\text{'Men'},\text{'Sports'}) \wedge i\_class \in (\text{'sports-apparel'},\text{'sailing'}))$ and
$\mathbb{A} : \{i\_category, i\_brand, s\_store\_name, s\_company\_name, d\_moy\}$.

Note that there are several attributes in the projection set, and both conjunctive and disjunctive predicates in the filter condition.

When the same experiments were carried out with Hydra, we found that typically over 90% of the constraints had a relative error of greater than 90%. Turning our attention to DataSynth, we also generated a customized workload from the TPC-DS benchmark, comprising of only single attribute projection and filter constraints to suit DataSynth's restricted environment. Even for this simplified scenario, we found several cases, where the LP solution obtained from DataSynth was *inconstructible*. An example illustration showcasing this fundamental problem is available in [21].

Due to this clear inability of both DataSynth and Hydra to produce data that satisfies projection-compliant constraints, we restrict our attention to PiGen in the rest of this section.

10.2 Generated Data

We now show a concrete example of how the data generated by PiGen satisfies the input PICs. Consider the following PIC from the Census workload on the Persons table:

$$\langle 18 \leq Age \leq 85 \wedge Relationship = \text{'Spouse'} \wedge PUMA = 822, (Age, Sex), 205, 4 \rangle$$

A snippet of the generated table is shown in Table 4. Here, the first four rows in the (Age, Sex) columns are repeated in round-robin fashion, while the remaining attributes have a fixed constant value, for producing the first 205 rows. Then, the subsequent rows (206th row onwards) in the table are assigned values that do not satisfy the above constraint.

Table 4: Sample Rows produced for persons Table

Age	Sex	Relationship	PUMA	Tenure
18	M	Spouse	822	Rented
25	F	Spouse	822	Rented
36	M	...	...	...
68	M	...	...	...
Repeated in Round Robin		Spouse	822	Rented
(Row # 206) 76	F	Parent	100	Owned
...	...	...	...	...

10.3 Time and Space Overheads

We now turn our attention to PiGen's computational and resource overheads. The summary construction times and sizes for various tables across workloads are reported in Table 5. We see here that the construction times range from a couple of seconds to a few tens of minutes. From a deployment perspective, these times appear acceptable since database generation is usually an offline activity. Moreover, the summary sizes are minuscule, within a few 100 KBs.

Drilling down into the summary production time, which is typically in the order of a few minutes, we find that virtually all of it is consumed in the LP solving stage. In fact, the collective time spent by the other stages was usually less than *ten seconds*. These results highlight the need for minimizing the number of LP variables, since the solving time is largely predicated on this number. To obtain a quantitative understanding, we report the sizes of the intermediate results at various pipeline stages in Table 6 – specifically, the table shows the number of FBs, RBs, and CPBs created by PiGen. We see here that there is a huge jump in the number of regions from the initial FB to the final CPBs, testifying that the workloads have considerable overlaps among their constituent PICs, representing "tough-nut" scenarios wrt projection. An exception to this observation is the persons table from Census dataset, where even though the maximum degree for a vertex in the Division graph was 72 (Table 3), the overlaps between PICs are limited as also indicated by the average degree which is less than 2.

Table 5: Overheads

Table	Summary	
	Time	Size
SS	21 min	58 kB
CS	32 min	117 kB
WS	15 min	64 kB
INV	2 s	13 kB
MK	2 min	15.5 kB
CI	41 s	13.6 kB
MC	3.6 min	27.7 kB
P	30 min	416 kB

Table 6: Block Profiles

Table	Cardinality of		
	FBs	RBs	CPBs
SS	74	88	132662
CS	139	141	165936
WS	119	132	73929
INV	11	16	41
MK	30	32	30083
CI	278	301	14386
MC	187	203	42835
P	1193	1529	7170

We also evaluated the time taken to flag infeasibility by PiGen for the cases where the input workload itself has infeasible PICs. In our experience, this situation was usually caught within a few minutes. As a case in point, on adding an infeasible constraint to the 220 PICs set for CENSUS data, the error was flagged in 3 minutes.

The table summaries can be used to either dynamically generate tuples during query processing, or produce materialized instances. Representative generation times are reported in Table 7, and we see that even a huge table such as SS, with close to 3 billion records, is generated within just a few minutes.

Table 7: Tuple Generation Time

Table	# Rows	Tuple Gen. Time	Table	# Rows	Tuple Gen. Time
SS	2.9 bn	4 min	WS	0.72 bn	8 seconds
CS	1.4 bn	1.5 min	INV	0.78 bn	9 seconds

10.4 Scalability Profile

Data Scale. The time and space overheads incurred to produce table summaries are intrinsically *data-scale-free*, i.e., they do not depend on the generated size. We explicitly verified this property by running PiGen over 10 GB, 100 GB and 1 TB versions of TPC-DS.

Workload Scale. The time and space requirements with increasing number of PICs is shown in Figures 5(a) and 5(b), respectively, for the Census workload. The figures highlight that the memory consumption is relatively stable and manageable (few GB) across

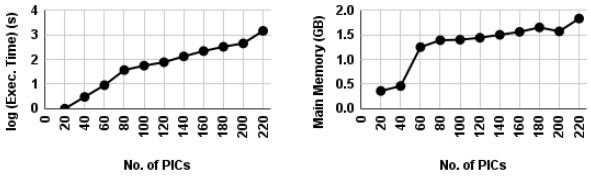

Figure 5: (a) Execution Time (b) Memory Usage

the spectrum, but that time scalability can be a limitation for workloads beyond a certain complexity (Figure 5(a) is on a log scale).

10.5 Workload Decomposition

We now turn our attention to intersecting workloads, which require the pre-processing step of workload decomposition. To model this scenario, we added intersecting PICs to the TPC-DS workload suite, with the final workloads having the following PIC distributions: SS (52 PICs), CS (28 PICs), WS (29 PICs), and INV (8 PICs).

We evaluated PiGen for these four tables and the results are shown in Table 8. We observe that despite using an approximate vertex coloring algorithm, the partitioning led to at most 6 sub-workloads for ensuring internal compatibility. Interestingly, the aggregate summary generation times are extremely small, completing in just a few seconds, and much lower than the corresponding numbers for the TPC-DS compatible suite in Table 5. At first glance, this might appear surprising given that the intersecting version is more complex in nature – the reason is that due to workload decomposition, an array of databases is produced with low individual production complexity, whereas a single unified database is produced for the compatible case. From a deployment perspective, it is preferable to generate the smallest number of databases, and therefore we would always strive to minimize the decomposition.

Finally, we also verified the quality of the approximation algorithm for decomposition. That is, how far is the obtained number of sub-workloads from the actual minimum count. To assess this, we implemented the exponential algorithm that computes the true minimum number of sub-workloads and in the cases where this exhaustive algorithm could be evaluated, we found that the approximation algorithm returned the same count as the optimal.

Table 8: Workload Decomposition

Table	Sub-Workload Sizes	Aggregate Summary Time	Aggregate Summary Size
SS	13,11,8,7,7,6	14 s	135 kB
CS	14,5,5,4	12 s	69 kB
WS	12,10,7	7 s	58 kB
INV	6,2	3 s	16 kB

11 CONCLUSIONS

Synthetic data generation from a set of cardinality constraints has been strongly advocated in the contemporary database testing literature. PiGen expands the scope of the supported constraints to include, for the first time, the general Projection operator. The primary challenges in this effort were tackling dependencies within a projection subspace and across different projection subspaces. By using a combination of workload decomposition and symmetric refinement, dependencies across various projection subspaces were handled. Within a projection subspace, union was converted to summation via division of the space. Further, an optimal division strategy was presented to construct efficient LP formulations of the constraints. The experimental evaluation on real-world and synthetic benchmarks indicated that PiGen successfully produces generation summaries with viable time and space overheads.

Currently, PiGen deems any exact solution to the LP as satisfactory for database generation. This choice could be materially improved in two ways: 1) By using approximation algorithms that sacrifice constraint accuracy to a limited extent to achieve better workload scalability; and 2) By preferentially directing the LP solver towards solutions with reduced sparsity so as to improve the robustness of the generated database to future unseen queries.

A PROOF OF LEMMA 9.1

We briefly discuss the proof for Lemma 9.1, which is split into two parts: (a) The LP constructed for a feasible compatible workload $\mathbb{C}$ is always satisfiable; (b) Given any LP solution, data can be always be constructed from it, and this data will satisfy $\mathbb{C}$.

Part (a): Given workload feasibility, there exists at least one instance T of the table that satisfies $\mathbb{C}$. Further, due to compatibility, $\mathbb{C}$ is modeled in a single LP. Say T does not satisfy this LP. This implies T does not satisfy at least one of the Explicit or Sanity constraints. If T violates an Explicit constraint, then it does not satisfy at least one input PIC. This is because each input PIC is modeled using two Explicit constraints that ensure the data satisfies the PIC. Further, there cannot be a physical table that violates any Sanity constraint due to its inherent nature. Hence, T satisfies all the Sanity constraints as well. Therefore, by contradiction, we can conclude that T satisfies the LP – in fact, the LP gives the *necessary* conditions for data generation adhering to the workload. This implies that for feasible workloads, the LP is satisfiable.

Part (b): For a particular PAS $\mathbb{A}$, the Sanity constraints ensure that for each populated RB, the total tuple count in the RB is at least the number of distinct rows along $\mathbb{A}$, and the distinct row count is positive. Hence, the data along each projection subspace is generated easily. Further, since RB is symmetric in nature, data across its different projection subspaces can be generated independently and concatenated. Therefore, any LP solution is *sufficient* for data generation. Since, each PIC is modelled in the LP using the Explicit constraints, the generated data is compliant with $\mathbb{C}$.

ACKNOWLEDGMENTS

We thank Srikanta Tirthapura for technical advice on the theoretical aspects of our study. We thank Shweta Patwa and Ashwin Machanavajjhala for providing us with the Census dataset and workload. The work of Anupam Sanghi was supported by an IBM PhD Fellowship Award.

REFERENCES

[1] [n.d.]. Dagstuhl Seminar 21442. Ensuring the Reliability and Robustness of Database Management Systems. https://www.dagstuhl.de/en/program/calendar/semhp/?semnr=21442

[2] [n.d.]. JOB Benchmark. https://github.com/gregrahn/join-order-benchmark

[3] [n.d.]. PostgreSQL. https://www.postgresql.org/docs/9.6/

[4] [n.d.]. TPC-DS. http://tpc.org/tpcds/

[5] [n.d.]. TPC-H. http://tpc.org/tpch/

[6] [n.d.]. Z3. https://github.com/Z3Prover/z3

[7] Alexander Alexandrov, Kostas Tzoumas, and Volker Markl. 2012. Myriad: Scalable and Expressive Data Generation. *PVLDB* 5, 12 (2012), 1890–1893.

[8] Arvind Arasu, Raghav Kaushik, and Jian Li. 2011. Data Generation using Declarative Constraints. In *Proc. of ACM SIGMOD Conf.* 685–696.

[9] Arvind Arasu, Raghav Kaushik, and Jian Li. 2011. DataSynth: Generating Synthetic Data using Declarative Constraints. *PVLDB* 4, 12 (2011), 1418–1421.

[10] Carsten Binnig, Donald Kossmann, and Eric Lo. 2007. Reverse Query Processing. In *Proc. of 23rd ICDE Conf.* 506–515.

[11] Carsten Binnig, Donald Kossmann, Eric Lo, and M Tamer Özsu. 2007. QAGen: Generating Query-Aware Test Databases. In *Proc. of ACM SIGMOD Conf.* 341–352.

[12] Béla Bollobás and Andrew Thomason. 1995. Projections of Bodies and Hereditary Properties of Hypergraphs. *Bulletin of the London Mathematical Society* 27, 5 (1995), 417–424.

[13] Nicolas Bruno and Surajit Chaudhuri. 2005. Flexible Database Generators. In *Proc. of 31st VLDB Conf.* 1097–1107.

[14] Amir Gilad, Shweta Patwa, and Ashwin Machanavajjhala. 2021. Synthesizing Linked Data Under Cardinality and Integrity Constraints. In *Proc. of ACM SIGMOD Conf.* 619–631.

[15] Jim Gray, Prakash Sundaresan, Susanne Englert, Ken Baclawski, and Peter J Weinberger. 1994. Quickly Generating Billion-Record Synthetic Databases. In *Proc. of ACM SIGMOD Conf.* 243–252.

[16] Imre Leader, Žarko Ranđelović, and Eero Raty. 2021. Inequalities on Projected Volumes. *SIAM Journal on Discrete Mathematics* 35, 3 (2021), 1678–1687.

[17] Maurizio Lenzerini and Paolo Nobili. 1987. On The Satisfiability of Dependency Constraints in Entity-Relationship Schemata. In *Proc. of 13th VLDB Conf.* 147–154.

[18] Yuming Li, Rong Zhang, Xiaoyan Yang, Zhenjie Zhang, and Aoying Zhou. 2018. Touchstone: Generating Enormous Query-Aware Test Databases. In *Proc. of USENIX ATC*. 575–586.

[19] Eric Lo, Nick Cheng, Wilfred W. K. Lin, Wing-Kai Hon, and Byron Choi. 2014. MyBenchmark: generating databases for query workloads. *The VLDB Journal* 23, 6 (2014), 895–913.

[20] Tilmann Rabl, Manuel Danisch, Michael Frank, Sebastian Schindler, and Hans-Arno Jacobsen. 2015. Just can't get enough: Synthesizing Big Data. In *Proc. of ACM SIGMOD Conf.* 1457–1462.

[21] Anupam Sanghi, Shadab Ahmed, and Jayant R. Haritsa. 2021. *Data Generation using Projection Constraints.* DSL/CDS Tech. Report TR-2021-03. Indian Institute of Science. https://dsl.cds.iisc.ac.in/publications/report/TR/TR-2021-03.pdf

[22] Anupam Sanghi, Rajkumar Santhanam, and Jayant R. Haritsa. 2021. Towards Generating HiFi Databases. In *Proc. of 26th DASFAA Conf.* 105–112.

[23] Anupam Sanghi, Raghav Sood, Jayant R. Haritsa, and Srikanta Tirthapura. 2018. Scalable and Dynamic Regeneration of Big Data Volumes. In *Proc. of 21st EDBT Conf.* 301–312.

[24] Anupam Sanghi, Raghav Sood, Dharmendra Singh, Jayant R. Haritsa, and Srikanta Tirthapura. 2018. HYDRA: A Dynamic Big Data Regenerator. *PVLDB* 11, 12 (2018), 1974–1977.

[25] Entong Shen and Lyublena Antova. 2013. Reversing Statistics for Scalable Test Databases Generation. In *Proc. of Sixth DBTest Workshop.* 1–6.

[26] Abraham Silberschatz, Henry F Korth, and S. Sudarshan. 2020. *Database System Concepts, Seventh Edition.* McGraw-Hill, New York.

[27] Zihan Tan and Liwei Zeng. 2019. On the Inequalities of Projected Volumes and the Constructible Region. *SIAM Journal on Discrete Mathematics* 33, 2 (2019), 694–711.